Published in final edited form as:
Dev Dyn. 2009 April ; 238(4): 853–863. doi:10.1002/dvdy.21899.

Deficiency screen identifies a novel role for beta 2 tubulin in salivary gland and myoblast migration in the *Drosophila* embryo

Rakhi Jattani[1,#], **Unisha Patel**[1], **Bilal Kerman**[#], and **Monn Monn Myat**[*]
Department of Cell and Developmental Biology Weill Medical College of Cornell University 1300 York Avenue New York, NY 10065 Phone: 212 746 1246 Fax: 212 746 8175

Abstract

The *Drosophila* embryonic salivary gland is an epithelial organ formed by the coordinated invagination and migration of primordial cells. To identify genes that regulate gland migration we performed a deficiency screen of the third chromosome. Here, we report on the analysis of the beta 2 tubulin isoform (β2t) that maps at 85D15. We show that in β2t mutant embryos, salivary glands did not complete their posterior migration and that migration of fusion competent myoblasts (FCMs) and longitudinal visceral muscle founder (LVMF) cells between the gland and CVM was delayed. We also demonstrate that gland migration defects correlate with reduced βPS and αPS2 integrin expression in the surrounding mesoderm and that β2t genetically interacts with genes encoding integrin αPS1 and αPS2 subunits. Our studies reveal for the first time that β2t is expressed in embryogenesis and that β2t plays an important role in salivary gland and myoblast migration, possibly through proper regulation of integrin adhesion proteins.

Keywords

Drosophila; salivary; gland; migration; morphogenesis; myoblast; mesoderm; tubulin; organ; epithelia

INTRODUCTION

During embryogenesis, cells move cohesively in large groups or individually as single cells. In cohesive migration, such as that of epithelial cells, migrating cells have to coordinate individual changes in cell adhesion and the cytoskeleton such that the entire group migrates as a collective unit. While much is known about single cell migration, largely from studies of tissue cultured cells, little is known of how cells achieve cohesive migration in a developing embryo. In addition to intracellular changes, migrating cells also have to coordinate their local interactions with surrounding tissues. For example, peripheral nerves in the embryonic mouse limb skin provide a template that determines the pattern of blood vessel branching via local secretion of VEGF (Mukouyama et al., 2002). Other examples that highlight the importance of tissue-tissue interactions in organ development include the role of the visceral mesoderm in morphogenesis of the *Drosophila* embryonic trachea (Boube et al., 2001), endoderm (Martin-Bermudo et al., 1999) and salivary gland (Bradley et al., 2003; Vining et al., 2005). Studies of organ morphogenesis using genetically tractable model systems such as *D. melanogaster* and *C. elegans* are beginning to identify genes involved in processes such as cell shape change and adhesion during cell migration.

[*]To whom correspondence should be addressed: mmm2005@med.cornell.edu.
[1]These authors contributed equally
[#]Current address: BCMB Graduate Program, Johns Hopkins University School of Medicine, Baltimore, MD, 21205.

However, little is known about how these cellular changes are coordinated spatially and temporally during cell migration in embryogenesis and the role tissue-tissue interactions play.

The *Drosophila* embryonic salivary gland provides an excellent system to study cell migration, in particular the role of intrinsic and extrinsic factors. The salivary gland is a pair of elongated tubes comprised of a single layer of epithelial cells surrounding a central lumen (Myat, 2005). In mid-embryogenesis, salivary gland primordial cells, which initially reside as two plates or placodes at the ventral surface of the embryo, invaginate into the interior of the embryo to form a pair of tubes. After invagination is complete, the distal tip of the salivary gland comes into contact with the overlying circular visceral mesoderm (CVM) (Bradley et al., 2003; Vining et al., 2005). Upon contact with the CVM the salivary gland makes a sharp posterior turn, beginning with the distal-tip, and migrates posteriorly until the entire gland is turned and lies with its longest axis in the anterior-posterior direction (Myat, 2005). The CVM provides both a physical barrier to prevent further dorsal movement of the gland and a substrate for posterior migration of the gland. In embryos mutant for genes that position visceral mesoderm precursors, such as *heartless*, *thickveins* and *tinman*, or genes required for CVM morphogenesis, such as Rho1 GTPase, integrity of the CVM and salivary gland migration are disrupted (Bradley et al., 2003; Xu et al., 2008).

Intimate association of the salivary gland with the CVM is necessary for making the sharp posterior turn that sets the gland on its migratory path; however, once the gland has made the turn it subsequently detaches from the CVM to continue migrating posteriorly. Detachment of the gland from the CVM occurs concomitantly with anterior migration of the longitudinal visceral muscle founder cells (LVMFs) that originate in the posterior mesoderm and migrate anteriorly along the midgut primordium and visceral mesoderm (Campos-Ortega and Hartenstein, 1997; Kusch and Reuter, 1999; Vining et al., 2005). Previous studies showed that gland detachment from the CVM is likely due to ingression of the migrating LVMFs between the gland and CVM. In embryos mutant for *jelly belly* or *biniou*, where LVMFs are properly specified but anterior migration is stalled, the gland does not detach from the undifferentiated VM and becomes overextended (Zaffran et al., 2001; Bradley et al., 2003; Vining et al., 2005). In addition to the CVM and LVMFs, salivary glands contact somatic mesoderm precursor cells, the fat body and the CNS during their migratory path (Vining et al., 2005). These studies highlight the important role tissue-tissue interactions play in salivary gland migration and reveal the importance of attachment to and detachment from the CVM in establishing the early migratory path of the gland.

To identify novel genes required for posterior turning and migration of the salivary gland, we performed a deficiency screen of the third chromosome. We identified 34 genomic intervals required for salivary gland migration. We further characterized the genomic interval 85D8-85E13 and show that the β2 tubulin (β2t) gene at 85D15, which encodes one of four β tubulin isoforms encoded by the *Drosophila* genome (Fackenthal et al., 1993) is expressed in numerous tissues during embryogenesis and regulates migration of the salivary gland, FCMs and LVMFs.

RESULTS

Third chromosome deficiency screen for gland migration mutants

Salivary gland cells invaginate during embryonic stage 11 to form a tubular organ (Fig. 1A). Once all gland cells have invaginated, the gland contacts the circular visceral mesoderm (CVM) on its distal-dorsal side and fusion competent myoblasts (FCMs) of the somatic mesoderm (SM) on its proximal-dorsal and ventral sides (Fig.1B). At this point, the gland turns posteriorly beginning with its distal tip (Fig. 1B). When the distal half of the gland has

turned posteriorly during stage 13 (C), FCMs began to migrate between the gland and the CVM such that by stage 14 (D), the dorsal side of the gland had dissociated from the CVM. Thus, posterior turning of the gland early in its migratory path began with attachment of the gland to the CVM and FCMs which is followed by migration of FCMs between the gland and CVM that ultimately severs the gland-CVM contact.

To identify novel genes required for salivary gland migration, we performed a deficiency screen of the collection of third chromosome deficiency lines available from the Bloomington Stock Center for defects in gland migration. Of the 100 third chromosome deficiency lines that delete approximately 92–95% of the polytene bands (Flybase), we identified 34 lines that showed defects in salivary gland migration when homozygous (Table I). We grouped the 34 deficiency lines into three phenotypic classes: class I: the salivary gland distal tip did not initiate turning and migration, as represented by *Df(3L)BSC12* homozygous embryos (Fig. 2B), class II: only the distal tip turned, represented by *Df(3R)BSC47* homozygous embryos (Fig. 2C) and class III: the distal half of the gland turned but the proximal half did not, represented by *Df(3L)XG5* homozygous embryos (Fig. 2D). We identified 13 deficiency lines with the class I no turning phenotype, 6 with the class II only tip turns phenotype and 15 with the class III incomplete turning phenotype.

β2 tubulin is required for salivary gland migration

We chose one of the deficiencies from class I, *Df(3R)by10* which deletes the 85D8-85E13 genomic interval for further analysis due to its severe and highly penetrant gland migration defect. In wild-type embryos, the distal tip of the gland has turned posteriorly by stage 12 (Fig. 2E) and by stage 14 (Fig. 2F) the entire gland has turned posteriorly. In contrast, in *Df(3R)by10* homozygous embryos, the distal tip of the salivary gland did not initiate the posterior turn at stage 12 and the gland failed to migrate posteriorly even at stage 14 (Fig. 2G and H). We observed an identical gland migration defect in embryos homozygous for *Df(3R)by416* which deletes the genomic interval 85D10-85E2 and *Df(3R)GB104* which deletes the 85D12-86E10 interval (data not shown). Since we were particularly interested in understanding the role of the microtubule and actin cytoskeleton in salivary gland migration, the first mutant line we tested was for beta 2 tubulin (β2t) which maps to 85D15 within the genomic intervals uncovered by *Df(3R)by10*, *Df(3R)by416* and *Df(3R)GB104*.

We characterized three different alleles of β*2t*, $\beta 2t^{N}$ which contains an EMS-induced stop codon resulting in the absence of any detectable protein product, $\beta 2t^{6}$ which is an EMS-induced amino acid substitution within an internal cluster of variable amino acids that has been identified as an isotype-defining domain in vertebrate β-tubulins and $\beta 2t^{DVR2}$ which is an EMS-induced amino acid substitution that destabilizes the protein (Fackenthal et al., 1995). The $\beta 2t^{6}$ mutant protein is as stable as the wild-type but assembles functionally defective microtubules (Kempheus et al., 1982; Kemphues et al., 1982; Fuller et al., 1988). Consistent with their molecular lesions, the $\beta 2t^{N}$ and $\beta 2t^{DVR2}$ alleles produced a salivary gland migration defect more severe than that of the $\beta 2t^{6}$ allele. In stage 12 embryos homozygous for $\beta 2t^{N}$, the distal tip of the salivary gland did not turn posteriorly in contrast to wild-type glands (Fig. 2I). By stage 14, when wild-type glands turned completely (Fig. 2F), only the distal half of $\beta 2t^{N}$ mutant glands turned posteriorly (Fig. 2J). In embryos mutant for $\beta 2t^{6}$, the gland began to migrate posteriorly at stage 12, as in wild-type embryos (Fig. 2E and K); however, by stage 14, only the distal half of the gland turned posteriorly in contrast to wild-type glands that turned completely (Fig. 2F and L). We measured the penetrance of the gland migration defect in $\beta 2t^{N}$ and $\beta 2t^{6}$ mutant embryos by counting glands that did not turn at all, only the tip turned, turned incompletely or turned completely (Fig. 2M). In stage 14 wild-type embryos, 94% of glands turned completely and 6% turned incompletely (Fig. 2M). In contrast, in $\beta 2t^{N}$ mutant embryos, 65% of glands turned completely, 25% turned incompletely, 2% of glands only turned at the distal tip and 5% of

glands did not turn at all (Fig. 2M). Similar results were obtained for β*2t*^{6} mutant embryos where 75% of mutant glands turned completely by stage 14 and in 25% of glands only the distal half turned (Fig. 2M). In stage 13 embryos, the β*2t*^{DVR2} allele caused gland migration defects of similar severity to β*2t*^{N} (Supplementary Figure 1). We also observed gland migration defects in embryos *trans*-heterozygous for β*2t*^{6} and β*2t*^{N} and embryos *trans*-heterozygous for these β*2t* alleles and *Df(3R)by10* (Supplementary Figure 1). From these data, we conclude that β*2t* is required for posterior migration of the embryonic salivary gland.

β2t RNA is expressed in numerous tissues during embryogenesis

Based on genetic and protein analyses β*2t* was previously reported to be expressed only during spermatogenesis where it is required for several distinct processes in spermatogenesis such as meiosis and assembly of the sperm tail axoneme (Kemphues et al., 1979; Kemphues et al., 1982; Kemphues et al., 1983; Bialojan et al., 1984; Fuller et al., 1987). Since our data showed that β*2t* was required for embryonic salivary gland migration we tested whether β*2t* transcripts were present during embryogenesis. We isolated mRNA from embryos predominantly between embryonic stages 12 and 15 and performed reverse transcription (RT)-PCR with primers specific to full-length β*2t*. We identified a single band of approximately 1Kb that corresponds to the β*2t* cDNA and did not detect any bands in the absence of RT (data not shown). Subsequently, we performed whole mount *in situ* hybridization (ISH) of wild-type embryos using anti-sense RNA probes to full-length β*2t*. At embryonic stages 12 and 14, β*2t* RNA was expressed in the developing circular visceral mesoderm (CVM) and somatic mesoderm (SM) (Fig. 3A and B). Since β*2t* was expressed in multiple tissues that could not be discerned clearly with conventional light microscopy, we analyzed β*2t* RNA expression by confocal imaging of embryos processed for fluorescent in situ hybridization (FISH). FISH analysis revealed that β*2t* was indeed expressed in the CVM and SM throughout embryogenesis but no transcript was detected in the salivary gland (Fig. 3C, D and E). We did not detect any expression with sense probes to full-length β*2t* (Fig. 3F). To confirm that the antisense RNA probe to β*2t* specifically detected the β*2t* isoform, we performed RNA ISH of *Df(3R)by416* embryos which delete the genomic interval to which the β*2t* gene maps. β*2t* RNA was expressed in *Df(3R)by416* heterozygous embryos (Fig. 3G); however, *Df(3R)by416* homozygous embryos showed low levels of expression in the SM (Fig. 3H). We reasoned that the low level of expression detected in *Df(3R)by416* homozygous embryos may be due either to maternal contribution or cross hybridization of the full-length β*2t* RNA probe to the β*3t* transcript with which it shares 88% similarity (Michiels et al., 1987; Rudolph et al., 1987). Thus, we reexamined β*2t* RNA expression in *Df(3R)by416* homozygous embryos using a probe that lacked the most N-terminal 162 nucleotides, the region of highest similarity between the two transcripts and detected no expression (Fig. 3I). Therefore, our data show that β*2t* is indeed expressed during embryogenesis, predominantly in mesoderm tissues, including the CVM and SM.

Detachment of the salivary glands from the CVM is delayed in β2t mutant embryos

Considering β*2t* was expressed in the CVM and the salivary gland is known to migrate along the CVM (Fig. 1; Bradley et al., 2003) we tested whether the β*2t* gland migration phenotype may in part be due to defects in gland-CVM interaction. In stage 12 wild-type embryos, salivary gland cells on the dorsal side of the distal tip contact the overlying CVM as the gland turns to migrate posteriorly (Fig. 4A). By stage 13, the distal half of the gland turned and migrated posteriorly along the CVM (Fig. 4B). Although dorsal cells in the mid-region of the gland continued to contact the CVM at stage 13, the distal tip gland cells detached from the CVM (Fig. 4B). By stage 15, the entire gland had turned posteriorly and had detached from the CVM (Fig. 4C). In some β*2t*^{N} mutant embryos with the most severe migration defect, the distal tip of the gland contacted the CVM but did not turn posteriorly

during stage 12 (Fig. 4D). The distal tip of β*2t* mutant glands began to migrate posteriorly during stage 13 (Fig. 4E); however, the glands were stalled at this point and remained associated with the CVM (Fig. 4F). By stage 16, $\beta 2t^{N}$ mutant glands were positioned more anteriorly than wild-type glands; however, their distal tips were no longer attached to the VM and $\beta 2t^{N}$ mutant glands contacted the evaginating gastric caecae like wild-type glands (Fig. 4G and H). These data demonstrate that detachment of the salivary gland from the CVM was delayed in β*2t* mutants and suggests that timely detachment of the gland from the CVM is essential for proper migration and final positioning of the gland.

β2t is required for FCM and LVMF migration between the salivary gland and CVM

Previous studies on salivary gland migration showed that detachment of the gland correlated with anterior migration of the longitudinal visceral muscle (LVM) founder cells (LVMFs) and that genes that disrupt LVMF anterior migration also disrupt gland detachment from the CVM (Vining et al., 2005). Thus, we hypothesize that β*2t* may regulate salivary gland migration through its requirement in LVM morphogenesis. To test this hypothesis, we stained wild-type and $\beta 2t^{N}$ mutant embryos for fusion competent myoblasts (FCMs) and LVM founder cells (LVMFs) that will form the LVM using antisera to Sticks and Stones (SNS) and Couch potato (Cpo), respectively. In wild type embryos at stage 12, the distal-tip of the gland contacted the CVM and dorsal gland cells located more proximally were in contact with SNS-positive FCMs that are part of the head mesoderm (Fig. 5A). As the gland continued to migrate during stage 13, a larger number of dorsal gland cells associated with the CVM (Fig. 5B). In addition, clusters of SNS-positive FCMs associated with the distal and proximal tips of the gland at this stage. In late stage 13, FCMs began to migrate between the gland and CVM at the distal and proximal tips of the gland concomitant with detachment of the distal tip of the gland from the CVM (Fig. 5C). By stage 14, the entire gland was surrounded by FCMs and the gland had detached completely from the CVM (Fig. 5D). In contrast, in stage 14 $\beta 2t^{N}$ mutant embryos, dorsal gland cells still contacted the CVM and FCMs at the distal and proximal tips of the gland had not migrated between the gland and CVM (Fig. 5E). The FCM migration defect was less severe in $\beta 2t^{6}$ mutant embryos compared to $\beta 2t^{N}$ mutant embryos; we observed a few FCM cells had migrated between the gland and CVM and the gland partially detached from the CVM in $\beta 2t^{6}$ mutant embryos (Fig. 5F).

In addition to delayed migration of FCMs between the gland and the CVM (Fig. 5), β*2t* was also required for migration of LVMFs between the gland and the CVM. In wild-type embryos at stage 12, LVMFs, which originate in the posterior mesoderm, had migrated along the CVM to reach the distal tip of the gland (Fig. 6A). By stage 13, the anterior most LVMFs have migrated approximately half the length of the gland between the gland and the CVM, severing the gland-CVM contact (Fig. 6B). In contrast, in stage 13 $\beta 2t^{N}$ mutant embryos, LVMFs migrated anteriorly to the distal tip of the gland but failed to migrate between the gland and CVM (Fig. 6C). Despite the delay in LVMF migration, the LVM still formed normally in $\beta 2t^{N}$ mutant embryos as evidenced by staining for FasIII in stage 17 wild-type and mutant embryos (data not shown).

β2t is required for integrin expression in the mesoderm

One mechanism by which the surrounding mesoderm contributes to salivary gland migration is through integrin mediated cell adhesion between the migrating gland and the mesoderm. In embryos mutant for *inflated*, which encodes the αPS2 integrin subunit or *multiple edematous wings* (*mew*), which encodes the αPS1 integrin subunit, or *myospheriod* which encodes the βPS subunit, salivary glands fail to turn and migrate posteriorly in a manner similar to that in β*2t* mutant embryos (Bradley et al., 2003). To test whether the β*2t* gland migration defect could be due in part to defects in integrin function we stained wild-type and

β2t^N mutant embryos for βPS and αPS2. In stage 11 wild-type salivary glands that have not turned yet to migrate posteriorly, βPS (Figure 7A) and αPS2 (Figure 7C) integrin subunits were localized in discrete clusters at sites of contact between the distal gland cells and the adjacent somatic mesoderm (SM) (Figure 7A, A', C and C', arrows). In contrast, in β2t^N mutant glands that have not turned posteriorly, βPS (Figure 7B) and αPS2 (Figure 7D) integrin subunits were markedly absent from contact sites between the distal gland cells and the adjacent SM (Figure 7B, B', D and D', arrows). Moreover, β2t^N mutant embryos showed decreased βPS and αPS2 integrins in the CVM compared to wild-type embryos (Figure 7). In support of our integrin localization data, we found that simultaneously reducing in half the gene dosage of β2t^N and if^{B2} or β2t^N and mew^6 also resulted in gland migration defects similar to that in β2t^N homozygous embryos. 30% of β2t^N and if^{B2} *trans*-heterozygous embryos showed gland migration defects (n=197 glands) whereas 36% of β2t^N and mew^6 *trans*-heterozygous embryos showed gland migration defects (n=163 glands). These data suggest that the failure of the salivary gland to turn and migrate posteriorly in β2t^N mutant glands may in part be due to the absence or reduction of integrin subunits in the surrounding mesoderm.

DISCUSSION

In this study we identified 34 genomic intervals required for salivary gland migration. We show that the β2 tubulin isoform located at 85D15 is required for salivary gland turning and for the timely detachment of the gland from the CVM which is important for posterior migration and final positioning of the gland. We demonstrate that in β2*t* mutant embryos, delayed detachment of mutant glands from the CVM occurred concomitantly with delayed migration of the FCMs and LVMFs between the gland and the CVM. These studies reveal that timely migration of surrounding FCM and LVMF and dissociation of the salivary gland from the CVM are important for salivary gland development. We further show that salivary gland and myoblast cell migration defects in β2*t* mutant embryos are accompanied by failure of αPS and βPS integrins to localize properly in the SM adjacent to the migrating gland.

Prior to contacting the CVM, the salivary gland first contacts the SM from when the gland cells invaginate until the end of embryogenesis. Furthermore, proper differentiation of the SM is required for gland invagination and posterior turning (Vining et al., 2005). In contrast to the SM, proper VM differentiation is not required for the initial phases of salivary gland migration (Bradley et al., 2003) but is required for positioning of the salivary gland in late embryogenesis (Vining et al., 2005). In embryos mutant for *tinman* (*tin*), *biniou* (*bin*), or *jellybelly* (*jeb*), which are required for VM differentiation, salivary glands remained associated with the CVM from stage 14 onward and were abnormally extended by the end of embryogenesis (Vining et al., 2005). Unlike *tin*, *bin* and *jeb* mutants, β2*t* mutant glands subsequently detached from the CVM and did not extend abnormally. Furthermore, the CVM was properly differentiated in β2*t* mutants in contrast to *tin*, *bin* and *jeb* mutants where some VM cells may adopt an SM cell fate (Azpiazu and Frasch, 1993; Weiss et al., 2001; Zaffran et al., 2001).

Based on the embryonic RNA expression pattern of β2*t*, it is possible that β2*t* is required for posterior migration of the salivary gland in a cell non-autonomous manner, perhaps in the FCM and LVMF cells for their timely migration between the gland and CVM that in turn disrupts the gland-CVM association. We cannot exclude the possibility that the salivary gland cells secrete a chemoattractant that promotes the FCMs and LVMFs to migrate between the gland and CVM. Alternatively, or in addition, β2*t* may function in the SM to promote proper integrin mediated adhesion between the gland cells and the SM that indirectly controls myoblast migration between the gland and CVM and subsequent detachment of the gland from the CVM.

A critical role for microtubules in morphogenesis and cell migration has long been recognized (Watanabe and Kaibuchi, 2005). For example, in migrating neurons, microtubules are concentrated in the extending membrane protrusions and around nuclei (Rivas and Hatten, 1995; Rakic et al., 1996; Schaar and McConnell, 2005). Furthermore, α-tubulin mutations inhibit neuronal migration in mice and result in lissencephaly in humans (Keays et al., 2007). In *Drosophila* border cells, the microtubule regulator, Stathmin is one of the genes upregulated during the migration of these cells (Borhgese et al., 2006). $\beta 2t^{N}$ mutant embryos are viable and even though myoblast migration was delayed, the visceral mesoderm did form normally. It is possible that β*2t* plays a redundant role in myoblast migration with β*3t* that is also expressed in the visceral and somatic muscle (Leiss et al., 1988; Kimble et al., 1989). Additional studies are necessary to determine how the β*2t* and β*3t* isoforms contribute to FCM and LVMF migration in the *Drosophila* embryo.

Our data suggest that one mechanism by which beta 2 tubulin controls salivary gland and myoblast migration is through expression of integrin subunits. Integrins have been shown to play a key regulatory role in the morphogenesis of a number of tissues in the *Drosophila* embryo. In particular, complementary integrin expression is required between the migrating visceral branch of the embryonic trachea and the surrounding mesoderm (Boube et al., 2001). Our studies highlight the important role of adhesion mediated tissue-tissue interactions in salivary gland development. Our third chromosome deficiency screen for salivary gland migration mutants provide us with a valuable set of genetic tools with which we can identify additional novel genes required for gland migration so that we may better understand the complex nature of organ migration and the role of tissue-tissue interactions in this process.

EXPERIMENTAL PROCEDURES

Drosophila strains

Canton-S flies were used as wild-type controls. The following strains were obtained from the Bloomington Stock Center and are described in FlyBase (www.flybase.bio.indiana.edu): third chromosome deficiency kit, $\beta 2t^{6}$, $\beta 2t^{N}$ and $\beta 2t^{DVR2}$.

Antibody staining of embryos

Embryo fixation and antibody staining were performed as previously described (Pirraglia et al., 2006). The following concentrations were used at the indicated dilution: rat dCreb-A antiserum at 1:10,000; mouse Crumbs antiserum (Developmental Studies Hybridoma Bank; Iowa City, IA) at 1:100; mouse β-galactosidase (β-gal) antiserum (Promega; Madison, WI) at 1:10,000 for whole-mount and 1:500 for fluorescence, mouse 2A12 antiserum (Developmental Studies Hybridoma Bank) at 1:5; mouse FasIII antiserum (Developmental Studies Hybridoma Bank) at 1:20; pre-absorbed SNS antiserum at 1:50 (a gift of Susan Abmayr); pre-absorbed Couch potato antiserum at 1:200 (a gift of Hugo Bellen); mouse βPS and αPS2 antisera at 1:100 and 1:5, respectively (Developmental Studies Hybridoma Bank). Appropriate biotinylated-(Jackson Immunoresearch Laboratories; Westgrove, PA), AlexaFluor488- or Rhodamine-(Molecular Probes; Eugene, OR) conjugated secondary antibodies were used at a dilution of 1:500. Whole-mount stained embryos were mounted in methyl salicylate (J.T. Baker; Phillipsburg, NJ) or Aquapolymount before visualization on a Zeiss Axioplan 2 microscope with Axiovision Rel 4.2 software (Carl Zeiss; Thornwood, NY). Thick (1 μm) fluorescent images were acquired on a Zeiss Axioplan microscope (Carl Zeiss, Thornwood, NY) equipped with LSM 510 for laser scanning confocal microscopy at the Rockefeller University Bio-imagining Resources Center (New York, NY).

Deficiency screen

Deficiency lines obtained from the Bloomington Stock Center were stained for dCREB-A. Embryos at stage 14 were scored for glands that completely turned, incompletely turned, only the distal tip turned or distal tip did not turn at all. For scoring of migration phenotypes, a minimum of 20 mutant glands was scored for each genotype reported.

RNA in situ Hybridization

Embryonic mRNA was detected by whole-mount *in situ* hybridization as previously described (Lehmann and Tautz, 1994). For fluorescent *in situ* hybridization, embryos were processed for detection by first blocking with Western Blocking Reagent (Roche; Mannheim, Germany), incubating overnight at 4°C with Sheep anti-DIG (Roche) and staining for the DIG epitope by antibody staining, replacing PBSTB with PBT.

Reverse Transcription and PCR Analysis

Total RNA was extracted according to manufacturer's instructions using the QIAshredder and RNeasy Mini kit from Qiagen. Reverse transcription (RT) was performed according to manufacturer's instructions using the OneStep RT-PCR kit from Qiagen. Briefly, RT was performed in a volume of 50 μL using RNA extracted from wild-type embryos with β2t-specific primers, β2t-1 (5' GGGCCAAGGGTCATTACACCG 3') and β2t-2 (5'CGCCCTCCTCATCGGACAG 3') generated by Invitrogen (Carlsbad, CA).

Supplementary Material

Refer to Web version on PubMed Central for supplementary material.

Acknowledgments

We thank the Bloomington Stock Center and the Developmental Biology Hybridoma Bank for fly stocks and antisera. We thank S. Abmayr and the Stowers Institue (Kansas) and H. Bellen for antisera. We thank past and present members of the Myat lab for their advice and support during this study. We thank M. Schober, D. Andrew and M. Baylies for their critical comments on the manuscript. This work was supported in part by Faculty Transition Award (K22) from the NIDCR to M.M.M.

Grant Sponsor: NIH, National Institute of Dental and Craniofacial Research (NIDCR) Grant number: K22-DE014702

REFERENCES

Azpiazu N, Frasch M. tinman and bagpipe: two homeo box genes that determine cell fates in the dorsal mesoderm of *Drosophila*. Genes & Development. 1993; 7:1325–1340. [PubMed: 8101173]

Bialojan S, Falkenburg D, Renkawitz-Pohl R. Characterization and developmental expression of β tubulin genes in *Drosophila melanogaster*. EMBO. 1984; 3:2543–2548.

Borhgese L, Fletcher G, Mathieu J, Atzberger A, Eades W, Cagan R, Rorth P. Systematic analysis of the transcriptional switch during migration of border cells. Dev Cell. 2006; 4:497–508.

Boube M, Martin-Bermudo MD, Brown NH, Casanova J. Specific tracheal migration is mediated by complementary expression of cell surface proteins. Genes & Development. 2001; 15:1554–1562. [PubMed: 11410535]

Bradley PL, Myat MM, Comeaux CA, Andrew DJ. Posterior migration of the salivary gland requires an intact visceral mesoderm and integrin function. Dev Biol. 2003; 257:249–262. [PubMed: 12729556]

Campos-Ortega, JA.; Hartenstein, V. The embryonic development of *Drosophila melanogaster*. Springer-Verlag; Heidelberg: 1997.

Fackenthal JD, Hutchens JA, Turner FR, Raff EC. Structural analysis of mutations in the Drosophila beta 2-tubulin isoform reveals regions in the beta-tubulin molecule required for general and for tissue-specific microtubule functions. Genetics. 1995; 139:267–286. [PubMed: 7705629]

Fackenthal JD, Turner RF, Raff EC. Tissue-specific microtubule functions in Drosophila spermatogenesis require the β2-tubulin isotype-specific carboxy terminus. Developmental Biology. 1993; 158:213–227. [PubMed: 8330671]

Fuller MT, Caulton JH, Hutchens JA, Kaufman TC, Raff EC. Genetic analysis of microtubule structure: a beta-tubulin mutation causes the formation of aberrant microtubules in vivo and in vitro. Journal of Cell Biology. 1987; 3:385–394. [PubMed: 3818786]

Fuller MT, Caulton JH, Hutchens JA, Kaufman TC, Raff EC. Mutations that encode partially functional beta-2 tubulin subunits have different effects on structurally different microtubule arrays. Journal of Cell Biology. 1988; 107:141–152. [PubMed: 3134362]

Keays D, Tian G, Poirier K, Huang G, Siebold C, Cleak J, Oliver P, Fray M, Harvey R, Molnar Z, Pinon M, Dear N, Valdar W, Brown S, Davies K, Rawling J, Cowan N, Nolan P, Chelly J, Flint J. Mutations in alpha-tubuln cause abnormal neuronal migration in mice and lissencephaly in humans. Cell. 2007; 128:45–57. [PubMed: 17218254]

Kempheus K, Kaufman T, Raff R, Raff E. The testis-specific beta-tubulin subunit in Drosophila melanogaster has multiple functions in spermatogenesis. Cell. 1982; 31:655–670. [PubMed: 6819086]

Kemphues K, Kaufman T, Raff R, Raff E. The testis-specific beta-tubulin subunit in Drosophila melanogaster has multiple functions in spermatogenesis. Cell. 1982; 31:655–670. [PubMed: 6819086]

Kemphues KJ, Raff EC, Kaufman TC. Genetic analysis of β2t, the structural gene for a testis-specific beta-tubulin subunit in Drosophila melanogaster. Genetics. 1983; 105:346–356.

Kemphues KJ, Raff RA, Kaufman TC, Raff EC. Mutation in a structural gene for a β-tubulin specific to testis in *Drosophila melanogaster*. Proc. Natl. Acad. Sci. USA. 1979; 76:3991–3995. [PubMed: 115008]

Kimble M, Incardona J, Raff EC. A variant -tubulin isoform of Drosophila melanogaster (− 3) is expressed primarily in tissues of mesodermal origin in embryos and pupae and is utilized in populations of transient microtubules. Dev Biol. 1989; 131:415–429. [PubMed: 2492243]

Kusch T, Reuter G. Functions for Drosophila brachyenteron and forkhead in mesoderm specification and cell signalling. Development. 1999; 126:3991–4003. [PubMed: 10457009]

Lehmann, R.; Tautz, D. *In situ* hybridization to RNA. Academic Press; San Diego: 1994. p. 755

Leiss D, Hinz U, Gasch A, Mertz R, Renkawitz-Pohl R. 3 tubulin expression characterizes the differentiating mesodermal germ layer during Drosophila embryogenesis. Development. 1988; 104:525–531. [PubMed: 3077351]

Martin-Bermudo MD, I. A-G, H. BN. Migration of the Drosophila primodial midgut cells requires coordination of diverse PS integrin functions. Development. 1999; 126:5161–5169. [PubMed: 10529432]

Michiels F, Falkenburg D, Muller AM, Hinz U, Otto U, Bellmann R, Glazer KH, Brand R, Bialojan S, Renkawitz-Pohl R. Testes-specific β2 tubulins are identical in *Drosophila melanogaster* and *D. hydei* but differ from the ubiquitous β1 tubulin. Chromosoma (Berl.). 1987; 95:387–395. [PubMed: 3119300]

Mukouyama Y, Shin D, Britsch S, Taniguchi M, Anderson D. Sensory nerves determin the pattern of arterial differentiation and blood vessel branching in the skin. Cell. 2002; 6:693–705. [PubMed: 12086669]

Myat MM. Making tubes in the Drosophila embryo. Dev Dyn. 2005; 232:617–632. [PubMed: 15712279]

Pirraglia C, Jattani R, Myat MM. Rac GTPase in epithelial tube morphogenesis. Developmental Biology. 2006; 290:435–446. [PubMed: 16412417]

Rakic P, Knyihar-Csillik E, Csillik B. Polarity of microtubule assemblies during neuronal cell migration. Proc. Natl. Acad. Sci. USA. 1996; 93:9218–9222. [PubMed: 8799181]

Rivas R, Hatten M. Motility and cytoskeletal organization of migrating cerebellar granule neurons. J Neurosci. 1995; 15:981–989. [PubMed: 7869123]

Rudolph DF, Kimble M, Hoyle HD, Subler MA, Raff EC. Three *Drosophila* beta-tubulin sequences: a developmentally regulated isoform (β3), the testes-specific isoform (β2), and an assembly-defective mutation of the testes-specific isoform (β2t8) reveal both an ancient divergence in metazoan isotypes and structural constraints for beta-tubulin function. Mol Cell Biol. 1987; 7:2231–2242. [PubMed: 3037352]

Schaar B, McConnell S. Cytoskeletal coordination during neuronal migration. Proc. Natl. Acad. Sci. USA. 2005; 102:13652–13657. [PubMed: 16174753]

Vining MS, Bradley PL, Comeaux CA, Andrew DJ. Organ positioning in Drosophila requires complex tissue-tissue interactions. Developmental Biology. 2005; 287:19–34. [PubMed: 16171793]

Watanabe T, Kaibuchi K. Regulation of microubules in cell migration. TRENDS in cell biology. 2005; 15:76–83. [PubMed: 15695094]

Weiss J, KL S, HH L, MP S. Jelly Belly: a Drosophila LDL receptor repeat-containing signal required for mesoderm migration and differentiation. Cell. 2001; 3:387–398. [PubMed: 11701128]

Xu N, Keung B, Myat M. Rho GTPase controls invagination and cohesive migration of the Drosophila salivary gland through Crumbs and Rho-kinase. Dev Biol. 2008; 321:88–100. [PubMed: 18585373]

Zaffran S, A K, HH L, M F. biniou (FoXF), a central component in a regulatory network controlling visceral mesoderm development and midgut morphogenesis in Drosophila. Genes & Development. 2001; 21:2300–2315.

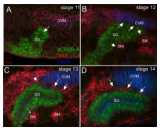

Figure 1. Salivary gland migration in the *Drosophila* embryo

In stage 11 wild-type embryos (A), the invaginating salivary gland (A, SG) does not contact the CVM. By stage 12 (B), the dorsal cells in the distal half of the gland (B, arrows) contact the CVM whereas the ventral cells contact the SM (B, arrowheads). During stage 13 (C), the salivary gland begins to detach from the CVM as fusion competent myoblasts (FCMs) migrate distal (C, large arrows) and proximal (C, arrowhead) to the gland but the gland remains in contact with the SM on the ventral side (C, small arrow). By stage 14 (D), the salivary gland no longer contacts the CVM and FCMs (D, arrows) have migrated in between the two tissues. All embryos shown were stained for dCREBA (green) to mark salivary gland nuclei, Sticks-and-stones (SNS) (red) to mark FCMs and FasIII (blue) to mark CVM.

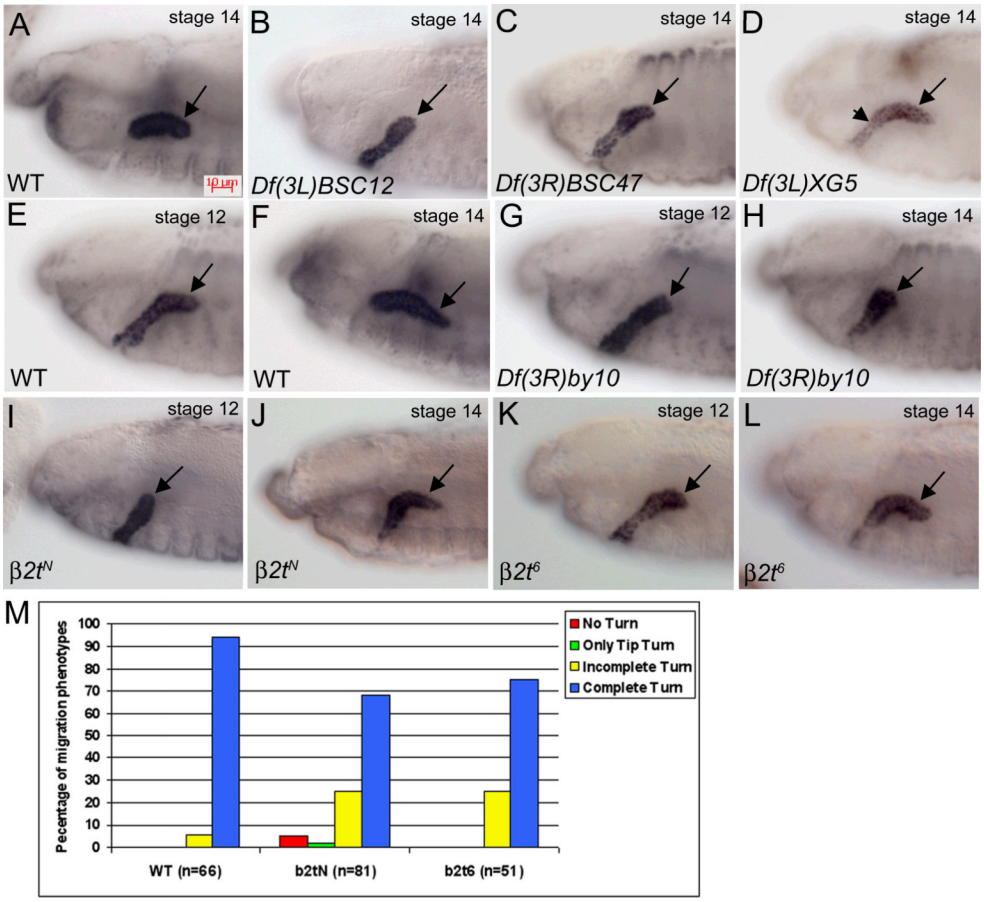

Figure 2. β*2t* is required for salivary gland migration

In wild-type embryos (A), the entire salivary gland has turned posteriorly by stage 14 (A, arrow). In embryos homozygous for *Df(3L)BSC12* (B), the gland does not turn, for *Df(3R)BSC47* (C) only the distal tip turns (C, arrow) and not the rest of the gland, and for *Df(3L)XG5* (D), the distal half (D, arrow) of the gland turns but the proximal half does not (D, arrowhead). In wild-type embryos at stage 12 (E), the distal tip of the gland has turned to migrate posteriorly and by stage 14 (F), the entire salivary gland (F, arrow) has completed its posterior turn. In embryos homozygous for *Df(3R)by10* (G and H) the gland does not migrate posteriorly (G and H, arrows). In embryos homozygous for $\beta 2t^N$ (I and J), the distal tip has not turned by stage 12 (I, arrow) and by stage 14 only the distal half of the gland has turned posteriorly (J, arrow). In embryos homozygous for $\beta 2t^6$ (K and L), the distal tip has turned by stage 12 (K, arrow) but by stage 14 only the distal half of the gland has turned posteriorly (L, arrow). (M) Stage 14 wild-type and mutant embryos were scored for gland migration defects. All embryos were stained for dCREB-A to mark gland nuclei and gland migration at stage 14 was scored for no turn, only tip turn, incomplete turn or complete turn of the gland. n in panel M represents number of glands scored.

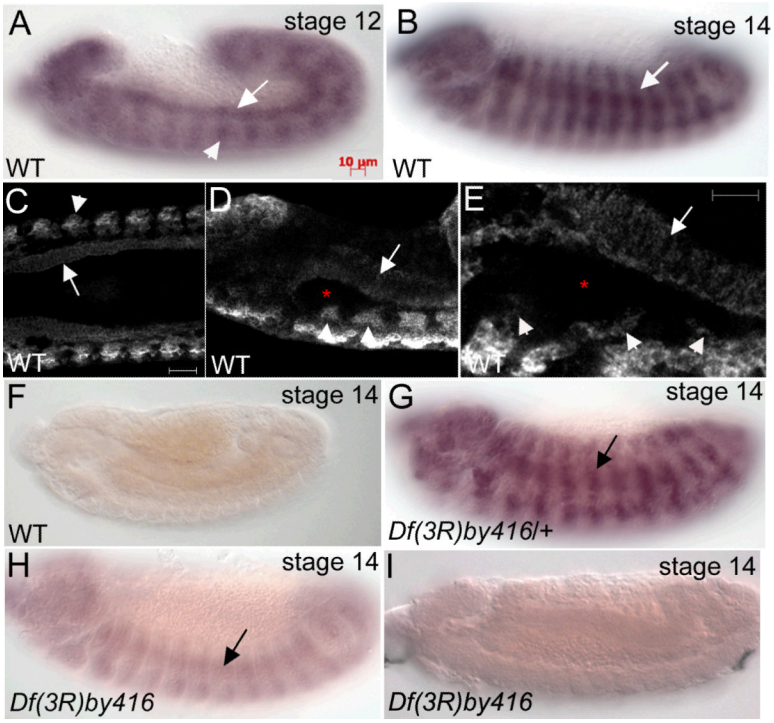

Figure 3. β*2t* is expressed in the mesoderm of *Drosophila* embryos

in situ hybridization of wild-type embryos (A−E) with full length antisense RNA probe to β*2t* shows expression in the circular visceral mesoderm (CVM) (A, arrow) and somatic mesoderm (SM) (A, arrowhead and B, arrow) at stages 12 (A) and 14 (B). One micron-thick confocal images of wild-type embryos (C, D and E) hybridized *in situ* with full length antisense RNA probes to β*2t* shows expression in the CVM (C, D and E, arrows) and SM (C, D and E, arrowheads) but not in the salivary gland (D and E, asterisks) at stage 14. *in situ* hybridization of wild-type embryos with sense RNA probe to β*2t* shows no expression (F). *Df(3R)by416* heterozygous embryos (G) hybridized *in situ* with full length β*2t* anti-sense RNA probes shows expression in the SM (G, arrow) and homozygous embryos show low levels of expression in the SM (H, arrow). *Df(3R)by416* homozygous embryos hybridized *in situ* with truncated β*2t* anti-sense RNA probes show no embryonic expression (H). Scale bars in C and E represent 10 μm.

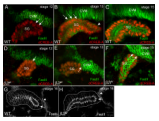

Figure 4. β*2t* is required for timely detachment of the migrating salivary gland from the CVM

In wild-type embryos (A, B and C), salivary gland cells on the dorsal side of the distal tip contact the overlying CVM and turn to migrate posteriorly at stage 12 (A, arrows). During stage 13 more proximal gland cells contact the CVM (B, arrows) and the distal tip of the gland (B, arrowhead) begins to detach from the CVM. By stage 15 (C), the entire gland is completely detached from the CVM. In stage 12 $\beta 2t^{N}$ mutant embryos (D, E and F), the distal tip of the gland contacts the CVM (D, arrow). During stages 13 (E) and 15 (F), the distal tip of the gland still contacts the CVM (E and F, arrows). In stage 16 wild-type (G) and $\beta 2t^{N}$ mutant embryos, the distal tip of the gland (G and H, arrows) contacts the evaginating gastric caecae (G and H, arrowheads). All embryos shown were stained for dCREB-A to mark the gland nuclei and FasIII to mark the CVM except for embryos in G and H that were stained only for FasIII.

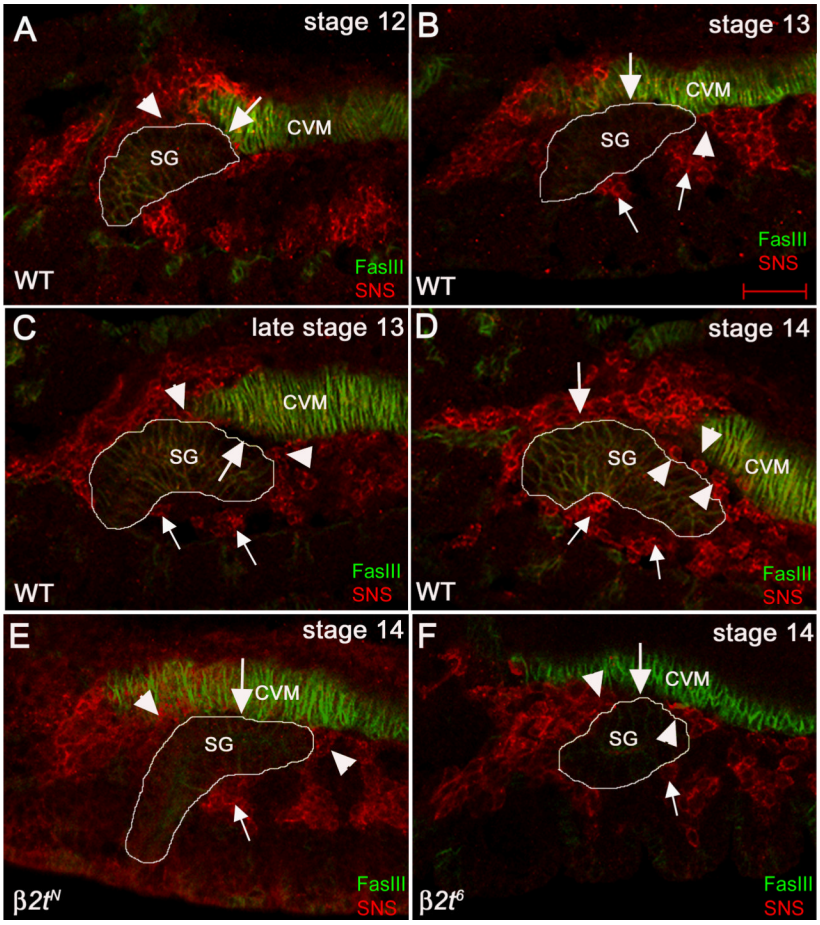

Figure 5. Migration of fusion competent myoblasts (FCMs) between the salivary gland and CVM is delayed in β*2t* mutant embryos

In wild-type embryos at stage 12 (A), dorsal cells at the distal tip of the gland contact the CVM (A, arrow) whereas dorsal cells more proximal to the distal tip contact FCMs (A, arrowhead). In embryonic stage 13, more dorsal gland cells contact the CVM (B, arrow) while the distal-most cells (B, arrowhead) and the ventral cells (B, small arrowheads) contact the FCMs. As posterior migration progresses during stage 13 (C), FCMs at the distal tip and the proximal-dorsal half of the gland (C, arrowheads) migrate in between the gland and the CVM creating a gap between the two tissues (C, arrow) whereas FCMs on the ventral side of the gland continue to contact the gland (C, small arrows). By stage 14 (D), the salivary gland (D, SG) has detached completely from the CVM and FCMs in the distal-half (D, arrowheads) and proximal half (D, arrow) have migrated in between the two tissues whereas FCMs on the ventral side of the gland continue to contact the gland (D, small arrows). In stage 14 $\beta 2t^{N}$ mutant embryos (E), the gland (E, SG) still contacts the CVM (E, arrow), FCMs (E, arrowheads) do not migrate between the two tissues and contact between the ventral side of the gland and SM is maintained (E, small arrow). In stage 14 $\beta 2t^{6}$ mutant embryos (F), the salivary gland (F, SG) partly contacts the CVM (F, arrow), FCMs (F, arrowheads) do not completely migrate between the gland and the CVM and contact between the ventral side of the gland and SM is maintained (F, small arrow). All embryos were stained for FasIII (green) to mark the CVM and salivary gland and SNS (red) to mark the FCMs. White lines outline the salivary gland.

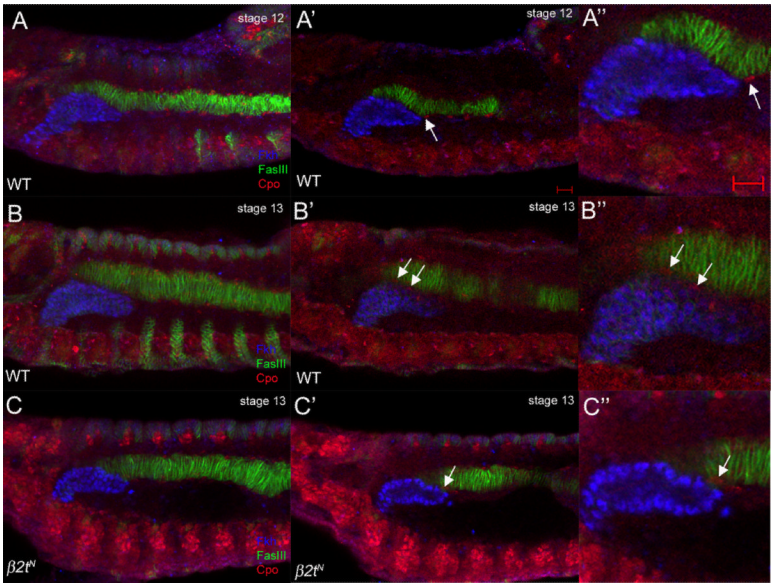

Figure 6. Migration of LVM founder cells between the CVM and salivary gland is delayed in β*2t* mutant embryos

In wild-type embryos at stage 12 (A, A' and A”), LVM founder cells (LVMFs) (A' and A”, arrows) migrate anteriorly dorsal and ventral to the CVM. During stage 13 in wild-type embryos (B, B' and B”), LVMFs (B' and B”, arrows) migrate between the CVM and salivary gland. In $\beta 2t^{N}$ mutant embryos at stage 13 (C, C' and C”), LVMFs have migrated anteriorly along the CVM (C' and C”, arrows) but have not migrated between the gland and CVM. Embryos in A–C were stained for Fkh (blue) to mark salivary gland nuclei, FasIII (green) for the CVM and Couch potato (red) to mark LVMFs. Scale bars in A' and A” represent 10 μm. A, B and C are projections of between 10 and 14 one micron-thick confocal optical sections whereas remaining panels depict a single one-micron thick optical section.

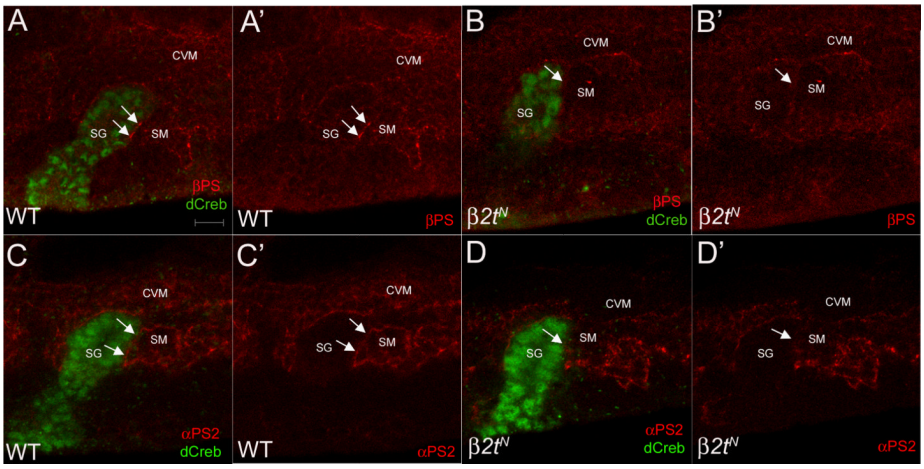

Figure 7. β2*t* is required for proper integrin expression in the mesoderm

In stage 11 wild-type salivary glands prior to posterior turning and migration (A and C), βPS (A and A', arrows) and αPS2 (C and C', arrows) localized to the contact sites between the distal gland cells and the adjacent SM (A, A', C and C', arrows). In stage 11 $\beta 2t^{N}$ mutant salivary glands prior to posterior turning (B and D), βPS (B and B', arrows) and αPS2 (D and D', arrows) did not localize to the contact sites between the gland and SM. Embryos in A and B were stained for βPS and dCreb-A whereas embryos in C and D were stained for αPS2 and dCreb-A. Scale bar in A represents 10 μm.

Table 1

Third chromosome deficiency lines with salivary gland migration defects

Deficiency	Break Points	Salivary Gland Migration Defect
Df(3L)emc-E12	61A-61D3	No Turning
Df(3L)Ar14-8	61C4-62A8	No Turning
Df(3L)ApRT32	62B1-62E3	No Turning
Df(3L)CH39	64-65B5	No Turning
Df(3L)BSC13	66B12-66D4	Incomplete Turning
Df(3L)AC1	67A2-67D7-13	No Turning
Df(3L)vin5	68A2-69A1	No Turning
Df(3L)ED4486	69C4-69F6	No Turning
Df(3L)BSC12	69F6-70A2	No Turning
Df(3L)XG5	71C2-72C1	Incomplete Turning
Df(3L)BSC8	74D3-75D5	Only Tip Turns
Df(3L)ED4799	76A1-76B3	Incomplete Turning
Df(3L)kto2	76B1-76D5	Only Tip Turns
Df(3L)XS533	76B4-77B1	No Turning
Df(3L)Ten-m-AL29	79C-79E8	Incomplete Turning
Df(3L)HD1	79D3-79F6	Incomplete Turning
Df(3L)BSC21	79E5-80A3	Incomplete Turning
Df(3L)ED5017	80A4-80C2	Only Tip Turns
Df(3R)BSC47	83B7-83D1	Only Tip Turns
Df(3R)Antp17	84A5-84D14	Only Tip Turns
Df(3R)p712	84D4-6--85B6	Incomplete Turning
Df(3R)BSC24	85C4-85D14	No Turning
Df(3R)by10	85D8-85E13	No Turning
Df(3R)BSC38	85F1-86C8	Incomplete Turning
Df(3R)T-32	86E2-87C7	Incomplete Turning
Df(3R)kar-Sz12	87B1-87C9	Incomplete Turning
Df(3R)D1-BX12	91F1-92D6	Incomplete Turning
Df(3R)BSC43	92F7-93B6	No Turning
Df(3R)e-R1	93B6-93D4	Only Tip Turns
Df(3R)23D1	94A3-94D4	Incomplete Turning
Df(3R)BSC55	94D2-94E6	No Turning
Df(3R)BSC56	94E1-94F2	Incomplete Turning
Df(3R)BSC42	98B1-98B5	Incomplete Turning
Df(3R)L127	99B5-99F1	Incomplete Turning